

# Compressed Sensing with Deep Image Prior and Learned Regularization

David Van Veen<sup>\*†</sup>  
vanveen@utexas.edu

Ajil Jalal<sup>\*†</sup>  
ajiljalal@utexas.edu

Eric Price<sup>‡</sup>  
ecprice@cs.utexas.edu

Sriram Vishwanath<sup>†</sup>  
sriram@austin.utexas.edu

Alexandros G. Dimakis<sup>†</sup>  
dimakis@austin.utexas.edu

December 14, 2024

## Abstract

We propose a novel method for compressed sensing recovery using untrained deep generative models. Our method is based on the recently proposed Deep Image Prior (DIP), wherein the convolutional weights of the network are optimized to match the observed measurements. We show that this approach can be applied to solve any differentiable inverse problem. We also introduce a novel learned regularization technique which incorporates a small amount of prior information, further reducing the number of measurements required for a given reconstruction error. Our algorithm requires approximately  $4-6\times$  fewer measurements than classical Lasso methods. Unlike previous approaches based on generative models, our method does not require the model to be pre-trained. As such, we can apply our method to various medical imaging datasets for which data acquisition is expensive and no known generative models exist.

## 1 Introduction

We consider the well-studied compressed sensing problem of recovering an unknown signal  $x^* \in \mathbb{R}^n$  by observing a set of noisy measurements  $y \in \mathbb{R}^m$  of the form

$$y = Ax^* + \eta.$$

Here  $A \in \mathbb{R}^{m \times n}$  is a known measurement matrix, typically generated with random independent Gaussian entries. Since the number of measurements  $m$  is smaller than the dimension  $n$  of the unknown vector  $x^*$ , this is an under-determined system of noisy linear equations and hence ill-posed. There are many solutions, and some structure must be assumed on  $x^*$  to have any hope of recovery.

Pioneering research [15, 8, 10] established that if  $x^*$  is assumed to be sparse in a known basis, a small number of measurements will be provably sufficient to recover the unknown vector in polynomial time using methods such as Lasso [42].

Sparsity in a known basis has proven successful for multiple signals of interest, but more complex models with additional structure have been recently proposed such as model-based compressive sensing [5] and manifold models [24, 23, 17]. Recently Bora et al. [7] showed that deep generative models can be used as excellent priors for images. They also showed that backpropagation can be used to solve the signal recovery problem by performing gradient descent in the generative latent space. Bora et al. [7] were able to reconstruct images with up to  $10\times$  fewer measurements compared to Lasso for a given reconstruction error. Compressed sensing using deep generative models was further improved in very recent work [44, 21, 28, 41, 19, 3]. Additionally a theoretical analysis of the nonconvex gradient descent algorithm [7] was proposed by Hand and Voroniski [22] under some assumptions on the generative model.

---

<sup>\*</sup>Equal contribution

<sup>†</sup>Department of Electrical and Computer Engineering, University of Texas at Austin

<sup>‡</sup>Department of Computer Science, University of Texas at Austin

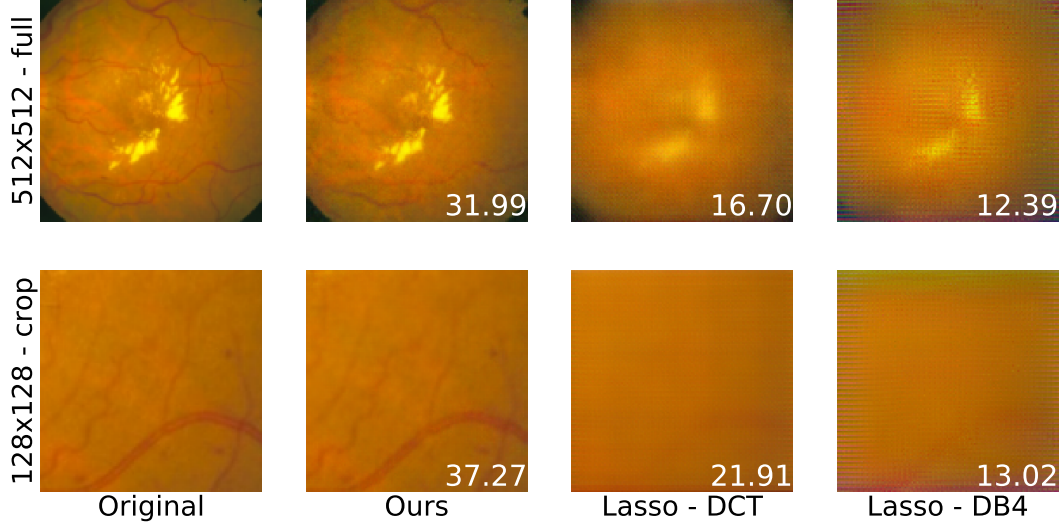


Figure 1: Comparison of our algorithm (CS-DIP) vs. baselines on RGB retinopathy medical images. We show a full 512x512 image (first row) and a 128x128 cropped portion of the same image (second row) to demonstrate finer details. For each row we show the original image (first column), our reconstruction (second column), and baseline reconstructions by Lasso in both the DCT basis and DB4 wavelet basis (third, fourth columns). Values in lower right of reconstructed images denote PSNR (dB). We recommend viewing these images in color.

Inspired by these impressive benefits of deep generative models, we chose to investigate the application of such methods for medical imaging, a canonical application of compressive sensing. A significant problem, however, is that all these previous methods require the existence of *pre-trained* models. While this has been achieved for various types of images (e.g. human faces of CelebA [32] via DCGAN [40]), it remains significantly more challenging for medical images. Instead of addressing this important problem in generative modeling, we found an easier way to circumvent it.

Surprising recent work by Ulyanov et al. [46] proposed Deep Image Prior (DIP), which uses *untrained* convolutional neural networks to perform inpainting and denoising. In DIP a convolutional neural network generator (e.g. DCGAN) is initialized with random weights; these weights are subsequently optimized to make the network produce an output as close to the target image as possible. This procedure is image-agnostic, using no prior information from other images. The prior is enforced only by the fixed convolutional structure of the generator network.

**Our Contributions:** In this paper we propose DIP for compressed sensing (CS-DIP). Our basic method is simple: we initialize a DCGAN generator with random weights and optimize them using gradient descent to make the network produce an output which *agrees with the observed measurements* as much as possible. We then introduce a novel *learned regularization* technique which further reduces the number of measurements required to achieve a given reconstruction error.

Our results show that we require approximately 4-6 $\times$  fewer measurements to obtain similar reconstruction error compared to Lasso. This benefit is not as significant as the 8-10 $\times$  obtained by Bora et al. [7], but we have the advantage of not requiring a pre-trained generative model. We can therefore apply our method to various medical imaging datasets for which no known generative models exist. We show further improved results using our learned regularization, which serves as a prior for optimal weights of the untrained network.

## 2 Background

### 2.1 Compressed Sensing: Classical Approaches

A classical assumption made in compressed sensing is that the vector  $x^*$  is  $k$ -sparse in some basis such as wavelet or discrete cosine transform (DCT). Finding the sparsest solution to an underdetermined linear system of equations is NP-hard in general; however, if the matrix  $A$  satisfies conditions such as the Restricted Eigenvalue Condition (REC) or Restricted Isometry Property (RIP) [9, 6, 15, 42], then  $x^*$  can be recovered in polynomial time via convex relaxations [45] or iterative methods. Another name for this problem is high-dimensional sparse linear regression, for which there is extensive literature regarding assumptions on  $A$ , numerous recovery algorithms, and variations of RIP and REC [6, 36, 1, 4, 33]. We use Lasso in both a DCT basis and a Daubechies wavelet basis as the baselines against which we compare our algorithm.

The goal of obtaining sufficient reconstructions with a small number of measurements can be motivated by understanding various applications of compressed sensing, such as communications and networking, analog-to-information converters, and RADAR. Imaging is another very common application. For instance consider the the single-pixel camera (SPC), where digital micro-mirrors provide linear combinations to a single light sensor. This sensor then uses compressed sensing algorithms to reconstruct a two-dimensional image [16]. Compressed sensing is also used in medical tomographic applications: particularly x-ray radiography, microwave imaging, magnetic resonance imaging (MRI), and computed tomography (CT) [50, 12, 34].

Measurements for medical imaging can be costly, time-consuming, and in some cases dangerous by exposing the patient to harmful radiation [39]. Hence there is great incentive to obtain quality reconstructions with fewer measurements. We address this need by using a network that is data-agnostic. This means it is not trained over a set of ground truth images, which would require a large amount of data. Instead our method only requires a portion of noisy measurements from the original image to achieve high quality reconstructions. This is demonstrated on medical data sets such as x-ray and retinopathy images.

### 2.2 Compressed Sensing: Deep Learning Approaches

While sparsity in some chosen basis is well-established, recent work has shown better empirical performance when neural networks are used [7]. This success is attributed to the fact that neural networks are capable of learning image priors from very large datasets [20, 29]. There is significant recent work on solving linear inverse problems using various deep learning techniques. Mardani et al. [35] propose recurrent generative models while Dave et al. [14] apply auto-regressive models.

Bora et al. [7] is the closest to our set-up. In this work the authors assume that the unknown signal is in the range of a pre-trained differentiable generative model like a Generative Adversarial Network (GAN) [20] or a variational autoencoder [29]. The recovery of the unknown signal is then obtained via gradient descent in the latent space to search for a generated signal that satisfies the measurements. This can be directly applied for linear inverse problems and more generally to any differentiable measurement process. Chang et al. [11] solve a problem similar to Bora et al. [7] but with a different optimization technique. Very recent work built upon the method of Bora et al. using amortized variational compressed sensing [21] and task-aware generator training [28].

The key point is that all this prior work requires pre-trained generative models. In contrast, as we discussed, our work applies DIP [46] which uses an untrained model and optimizes the network weights for linear measurements taken from an individual image. This means our unregularized method (CS-DIP) can be applied even if measurements from only one image are available. Our learned regularizer requires access to measurements from only a few (roughly 10 – 50) similar images to learn the prior distribution of the weights of network layers. This results in an informative prior using much less data than would be required to train a VAE or a GAN over a large image dataset.

## 3 Methods

Let  $x^* \in \mathbb{R}^n$  be the signal that we are trying to reconstruct,  $A \in \mathbb{R}^{m \times n}$  be the measurement matrix, and  $\eta \in \mathbb{R}^m$  be independent noise. Given the measurement matrix  $A$  and the observations  $y = Ax^* + \eta$ , we wish to reconstruct an  $\hat{x}$  that is close to  $x^*$ .

A generative model is a deterministic function  $G(z; w): \mathbb{R}^k \rightarrow \mathbb{R}^n$  which takes as input a seed  $z \in \mathbb{R}^k$  and a set of parameters (or “weights”)  $w \in \mathbb{R}^d$ , producing an output  $G(z; w) \in \mathbb{R}^n$ . These models have shown excellent performance generating real-life signals such as images [20, 29] and audio [47]. We investigate *deep convolutional* generative models, a special case in which the model architecture has multiple cascaded layers of convolutional filters [30]. In this paper we apply a DCGAN [40] model and restrict the signals to be images.

### 3.1 Compressed Sensing with Deep Image Prior (CS-DIP)

Our approach is to find a set of weights for the convolutional network such that the measurement matrix applied to the network output, i.e.  $AG(z; w)$ , matches the measurements  $y$  we are given. Hence we initialize an *untrained* network  $G(z; w)$  with some fixed  $z$  and solve the following optimization problem:

$$w^* = \arg \min_w \|y - AG(z; w)\|^2. \quad (1)$$

This is, of course, a non-convex problem because  $G(z; w)$  is a complex feed-forward neural network. Still we can use gradient-based optimizers for any generative model and measurement process that is differentiable. Ulyanov et al. observed that generator networks such as DCGAN are biased toward smooth, natural images due to their convolutional structure; thus the network structure alone provides a good prior for reconstructing images in problems such as inpainting and denoising [46]. Our finding is that this applies to general linear measurement processes. We restrict our solution to lie in the span of a convolutional neural network, and if a sufficient number of measurements  $m$  is given, we obtain an output such that  $x^* \approx G(z; w^*)$ .

Note that this method uses an untrained generative model and optimizes over the network weights  $w$ . In contrast previous methods such as that of Bora et al. [7] use a trained model and optimize in the latent  $z$ -space, solving  $z^* = \arg \min_z \|y - AG(z; w)\|^2$ . We instead initialize a random  $z$  and keep this fixed throughout the optimization process.

### 3.2 Learned Regularization

The methods of CS-DIP, as discussed above, rely only on linear measurements taken from one unknown image. We now investigate how a small amount of additional training data can be leveraged to obtain similar reconstruction with fewer measurements compared to CS-DIP. In this case training data refers to a set of measurements from additional ground truth images of a similar type, e.g. other x-ray images.

To leverage this additional information, we pose Eqn. (1) as a Maximum a Posteriori (MAP) estimation problem and propose a novel prior on the weights of the generative model. This prior then acts as a regularization term and penalizes the model toward an optimal set of weights  $w^*$ .

For a set of weights  $w \in \mathbb{R}^d$ , we model the *likelihood* of the measurements  $y = Ax, y \in \mathbb{R}^m$ , as a Gaussian distribution given by

$$p(y|w) = \frac{1}{\sqrt{(2\pi)^m \lambda}} \exp \left( -\frac{\|y - AG(z; w)\|^2}{2\lambda} \right), \quad (2)$$

and the prior on the weights  $w$  as a Gaussian given by

$$p(w) = \frac{1}{\sqrt{(2\pi)^d |\Sigma|}} \exp \left( -\frac{1}{2} (w - \mu)^T \Sigma^{-1} (w - \mu) \right), \quad (3)$$

where  $\mu \in \mathbb{R}^d$  and  $\Sigma \in \mathbb{R}^{d \times d}$ .

In this setting we want to find a set of weights  $w^*$  that maximize the posterior on  $w$  given  $y$ , i.e.,

$$\begin{aligned} w^* &= \arg \max_w p(w|y), \\ &= \arg \max_w \frac{p(y|w)p(w)}{p(y)}, \\ &\equiv \arg \min_w \|y - AG(z; w)\|^2 + \lambda (w - \mu)^T \Sigma^{-1} (w - \mu). \end{aligned} \quad (4)$$

This gives us the regularization term

$$R(w) = (w - \mu)^T \Sigma^{-1} (w - \mu), \quad (5)$$

where the coefficient  $\lambda$  in Eqn. (4) controls the strength of the prior.

Notice that when  $\mu = 0$  and  $\Sigma = I_{d \times d}$ , this regularization term is equivalent to  $\ell_2$ -regularization. Thus this method can be thought of as a more strategic version of standard weight decay.

### 3.2.1 Learning the Prior Parameters

In the previous section we introduced the regularization function:

$$R(w) = (w - \mu)^T \Sigma^{-1} (w - \mu).$$

However we do not yet know good values for  $(\mu, \Sigma)$  that will give high quality reconstructions. For a fixed set of measurements  $m$  and a measurement matrix  $A$ , we now propose a way to estimate  $(\mu, \Sigma)$  such that we can incorporate prior knowledge of the network weights.

Assume we have a set of measurements  $S_Y = \{y_1, y_2, \dots, y_K\}$  from  $K$  different images  $S_X = \{x_1, x_2, \dots, x_K\}$ , each obtained with a different measurement matrix  $A$ . For each measurement  $y_i, i \in \{1, 2, \dots, K\}$ , we run CS-DIP to solve the optimization problem in Eqn. (1) and obtain an optimal set of weights  $W^* = \{w_1^*, w_2^*, \dots, w_K^*\}$ . Note that when optimizing for the weights  $W^*$ , we only have access to the measurements  $S_Y$ , not the ground truth  $S_X$ .

The number of weights  $d$  in deep networks tends to be very large. As such, learning a distribution over each weight, i.e. estimating  $\mu \in \mathbb{R}^d$  and  $\Sigma \in \mathbb{R}^{d \times d}$ , becomes intractable. We instead use a layer-wise approach: with  $L$  network layers, we have  $\mu \in \mathbb{R}^L$  and  $\Sigma \in \mathbb{R}^{L \times L}$ . Thus each weight within layer  $l$  is modeled according to the same  $\mathcal{N}(\mu_l, \Sigma_{ll})$  distribution. For simplicity we assume  $\Sigma_{ij} = 0 \forall i \neq j$ , i.e. that network weights are independent across layers. The process of estimating statistics  $(\mu, \Sigma)$  from  $W^*$  is described in Algorithm (1), where we find different  $(\mu, \Sigma)$  for each measurement number  $m$ .

We use this learned  $(\mu, \Sigma)$  in the regularization term  $R(w)$  from Eqn. (5) for reconstructing measurements of images. We refer to this technique as *learned regularization* and demonstrate its effects in Section 4.

### 3.2.2 Discussion

The proposed CS-DIP algorithm is data-agnostic if no regularization is used. That is, given measurements for any single unknown image  $x^* \in \mathbb{R}^n$ , we can search for good weights  $w^*$  such that the generator network produces an output which approximately satisfies these measurements. The goal of the learned regularizer is to show that a small amount of prior information can further reduce the number of required measurements. This prior only requires access to measurements from a small number of images (roughly 10 – 50). In contrast,

---

**Algorithm 1** Procedure to estimate  $(\mu, \Sigma)$  for a distribution over optimal network weights  $W^*$

---

**input** Set of optimal weights  $W^* = \{w_1^*, w_2^*, \dots, w_K^*\}$  obtained from  $L$ -layer CS-DIP network run over  $K$  images each with  $m$  measurements; number of samples  $S$ ; number of iterations  $T$ .

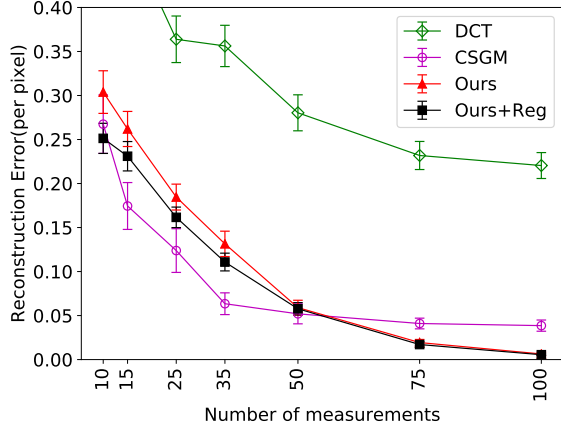
**output** mean vector  $\mu_m \in \mathbb{R}^L$ ; covariance matrix  $\Sigma_m \in \mathbb{R}^{L \times L}$ .

```

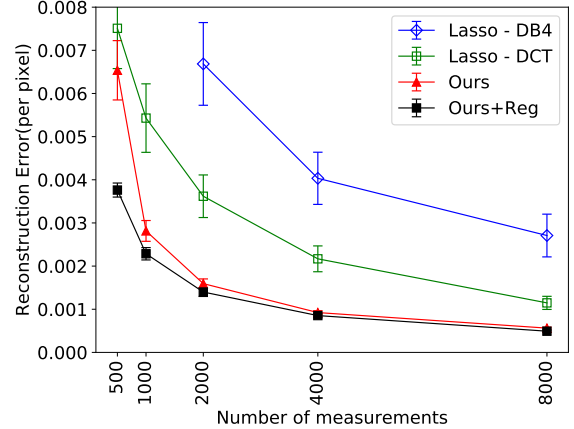
1: for  $t = 1$  to  $T$  do
2:   Sample  $k$  uniformly from  $\{1, \dots, K\}$ 
3:   for  $l = 1$  to  $L$  {for each layer} do
4:     Get  $v \in \mathbb{R}^S$ , a vector of  $S$  uniformly sampled weights from the  $l^{th}$  layer of  $w_k^*$ 
5:      $M_t[l, :] \leftarrow v^T$  where  $M_t[l, :]$  is the  $l^{th}$  row of matrix  $M_t \in \mathbb{R}^{L \times S}$ 
6:      $\mu_t[l] \leftarrow \frac{1}{S} \sum_{i=1}^S v_i$ 
7:   end for
8:    $\Sigma_t \leftarrow \frac{1}{S} M_t M_t^T - \mu_t \mu_t^T$ 
9: end for
10:  $\mu_m \leftarrow \frac{1}{T} \sum_{t=1}^T \mu_t$ 
11:  $\Sigma_m \leftarrow \frac{1}{T} \sum_{t=1}^T \Sigma_t$ 

```

---



(a) Results on MNIST (784 pixels)



(b) Results on Chest X-Rays (65536 pixels)

Figure 2: We compare the performance of our algorithm with baselines, plotting per-pixel reconstruction error (MSE) vs. number of measurements, where vertical bars indicate 95% confidence intervals. The black and red lines show reconstruction error obtained by our algorithm with and without learned regularization, respectively. For MNIST (2a) we are also able to compare with CSGM by Bora et al. [7]. CSGM outperforms our method for small number of measurements but requires a pre-trained generator for the sensed images. On the contrary our model can be applied to any type of image and delivers better performance when we have more than 50 measurements. For the chest x-ray dataset (2b), we could not compare to CSGM since no generative model is available for x-ray images. We expect that methods which leverage trained generative models will outperform our method, at least for small numbers of measurements.

other pre-trained models such as that of Bora et al. [7] require access to ground truth from a large number of similar images (tens of thousands for CelebA). If such a large dataset is available and if a good generative model can be trained on that dataset, we expect that methods which use pre-trained models [7, 21, 28, 35] can outperform our method. Our approach is instead more suitable for reconstructing problems where large amounts of data or good generative models are not readily available.

## 4 Experiments and Results

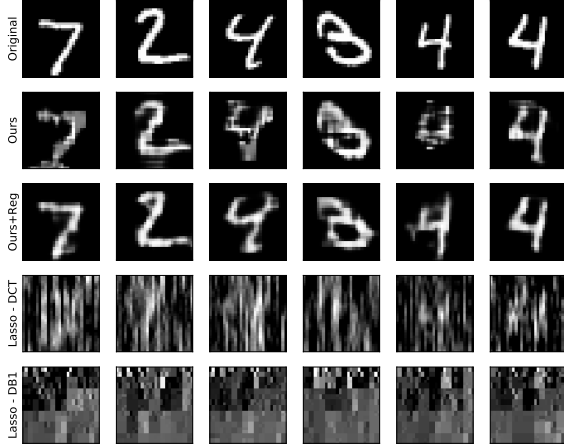
### 4.1 Experimental Setup

*Measurements:* As is standard in compressed sensing, the measurement matrices  $A \in \mathbb{R}^{m \times n}$  are created by sampling Gaussian I.I.D. random variables for each matrix entry, such that  $A_{i,j} \sim \mathcal{N}(0, \frac{1}{m})$ . Recall  $m$  is the number of measurements, and  $n$  is the number of pixels in the ground truth image.

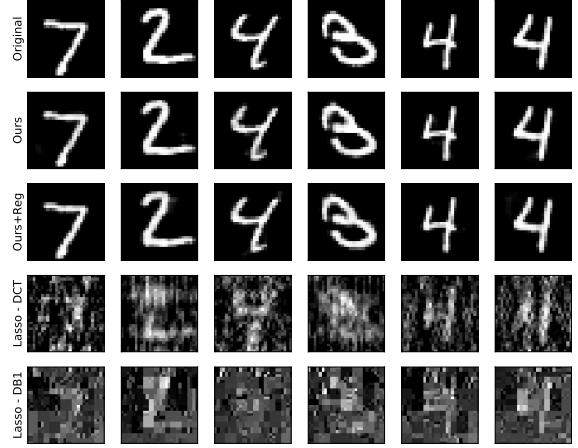
*Datasets:* We demonstrate our algorithm on both grayscale and RGB images. For grayscale we use the first 100 images in the test set of MNIST [31]. We also use 100 random images from the Shenzhen Chest X-Ray Dataset [27], selecting a 512x512 crop and then downsampling to 256x256 pixels. To evaluate our algorithm on RGB images, we use the Structured Analysis of the Retina (STARE) dataset [25] with both (1) 128x128 crops and (2) 512x512 crops downsized to 128x128 pixels.

*Metrics:* To quantitatively evaluate the performance of our algorithm, we use two different metrics. The first metric is per-pixel mean-squared error (MSE) between the reconstruction  $\hat{x}$  and true image  $x^*$ , i.e.  $\frac{\|\hat{x} - x^*\|^2}{n}$ . However, it is possible for blurry reconstructions to have low MSE [18]. Thus for a second metric, we use structural similarity (SSIM) [48] index, which measures perceived similarity between the original and reconstructed images.

*Optimizers:* To find a set of weights  $w^*$  that minimize Eqn. (1), we use a PyTorch [37] implementation of the RMSProp optimizer [43] with learning rate  $10^{-3}$  and momentum 0.9. We do 5 random restarts with 300 update steps per restart and pick the reconstruction with lowest error. For baseline reconstructions we use



(a) Results on MNIST,  $m = 50$



(b) Results on MNIST,  $m = 100$

Figure 3: Reconstruction results on MNIST for  $m = 50$  and  $m = 100$  measurements (of  $n = 784$  dimensional vector). We show original images (top row), reconstructions by our algorithm (second row), our algorithm with learned regularization (third row), and baseline reconstructions by Lasso in both the DCT basis and DB1 wavelet basis (bottom two rows).

the scikit-learn [38] implementation of Lasso with the contraction parameter yielding best results, which we found to be  $\alpha = 10^{-5}$ .

## 4.2 Results

We first discuss our algorithm (CS-DIP) compared to the Lasso baselines in both a DCT basis [2] and a Daubechies wavelet basis [13, 49]. Then in Section 4.2.4 we discuss the overall improvement delivered by our learned regularization technique.

### 4.2.1 MNIST

In Figure 2a we plot reconstruction error with varying number of measurements  $m$  of  $n = 784$ . This demonstrates that our algorithm, both with and without regularization, significantly outperforms Lasso DCT. We require roughly  $6\times$  fewer measurements than the Lasso baseline to achieve the same error. This also shows that, as expected, the pre-trained model of Bora et al. [7] outperforms our untrained algorithm for some values of  $m$ . In Figures 3a and 3b, we show reconstructions using our algorithm with and without learned regularization compared to Lasso. This demonstrates that our algorithm produces reasonable reconstructions with as few as 50 measurements, at which point Lasso produces indecipherable reconstructions. The reconstructed images for  $m = 200, 300, 400$  are in the appendix (Fig. 5, 6, 7).

### 4.2.2 Chest X-Rays

In Figure 2b we plot the reconstruction error with varying number of measurements  $m$  of  $n = 65536$ . On this dataset we also significantly outperform Lasso, which requires roughly  $4\times$  more measurements to achieve the same error. Figure 4 demonstrates reconstructions using our algorithm with and without learned regularization compared to Lasso. We observe that our algorithm produces reasonable reconstructions with as few as  $m = 2000$  measurements, while Lasso’s output is quite blurry. The reconstructed images for  $m = 1000, 4000, 8000$  are in the appendix (Fig. 8, 9, 10).

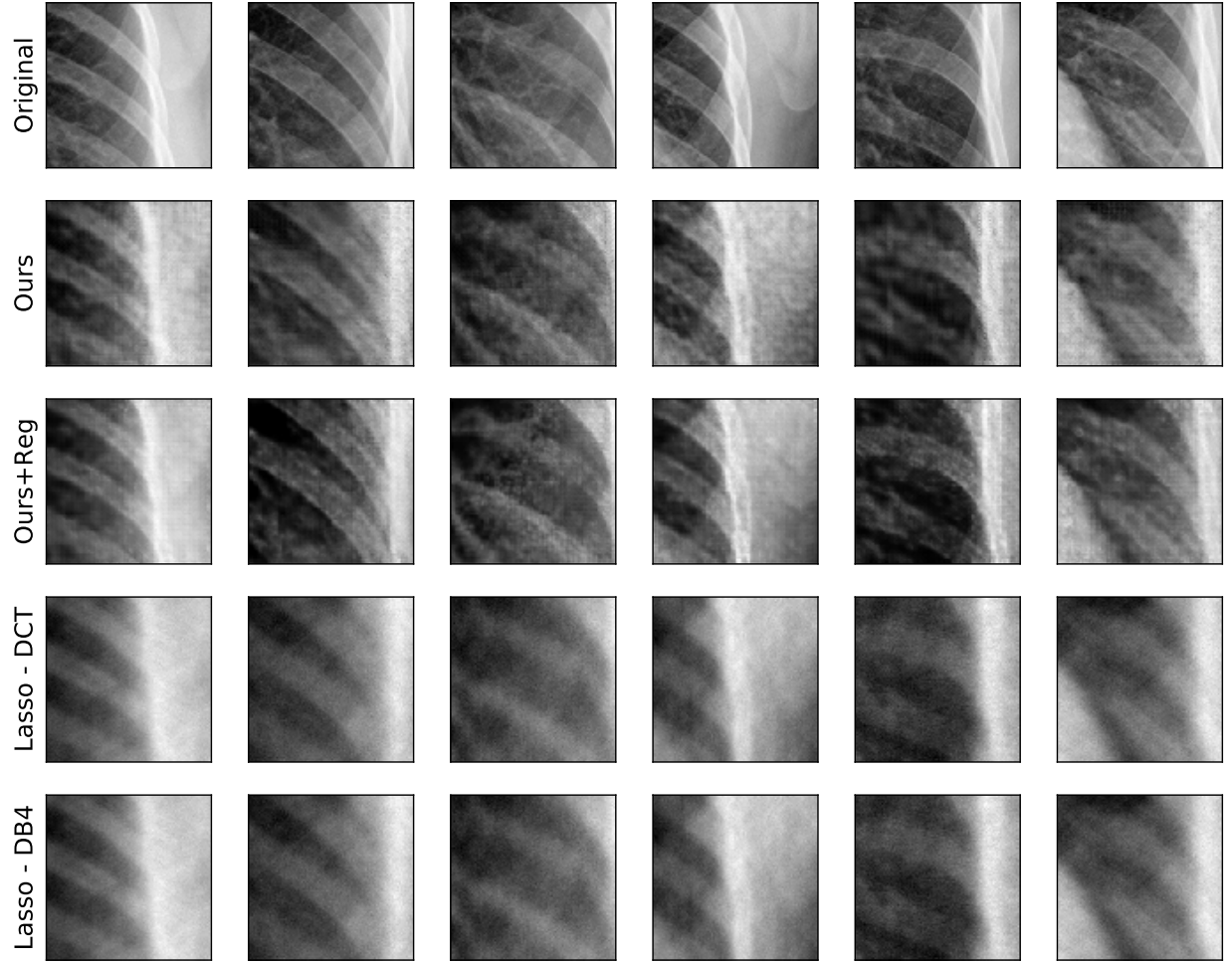


Figure 4: Reconstruction results on x-rays for  $m = 2000$  measurements (of  $n = 65536$  dimensional vector). We show original images (top row), reconstructions by our algorithm (second row), our algorithm with learned regularization (third row), and baseline reconstructions by Lasso in both the DCT basis and DB4 wavelet basis (bottom two rows).



$m$	CS-DIP	CS-DIP + Reg
500	.58	.71
1000	.72	.77
2000	.80	.82
4000	.86	.87
8000	.90	.91

Table 1: Average SSIM values obtained by our algorithm with and without learned regularization for varying number of measurements. The ground truth is a vector of size  $n = 65536$ .

### 4.2.3 Retinopathy

In Figure 1 we show reconstructions using our algorithm (CS-DIP) and Lasso. We see that our algorithm can reconstruct fine details in the retina scans, such as blood vessels and bright spots. Meanwhile for the same number of measurements, Lasso fails to produce a comprehensible image.

### 4.2.4 Learned Regularization

This learned regularization technique reduces error significantly for lower number of measurements, i.e.  $m = 10$  to  $50$  of  $n = 784$  for MNIST (Fig. 2a) and  $m = 500$  to  $2000$  of  $n = 65536$  for x-rays (Fig. 2b). We also demonstrate reconstructions with learned regularization for MNIST with  $m = 50, 100$  (Fig. 3a, 3b) and x-rays with  $m = 2000$  (Fig. 4). For certain values of  $m$ , these figures demonstrate that reconstructed images obtained using learned regularization are sharper and have fewer artifacts. For the case of  $m = 100$  on MNIST, however, there is not noticeable qualitative improvement. This finding is consistent with the quantitative results in Table 1, which shows that learned regularization results in significantly higher SSIM [48] only for lower values of  $m$ .

## 5 Conclusion

We demonstrate how to perform compressed sensing using untrained, randomly initialized convolutional neural networks. Our method requires  $4\text{-}6\times$  fewer measurements compared to the standard Lasso baselines. We further improve upon this through a novel learned regularization method which leverages prior belief on measurements from the underlying dataset.

One interesting extension of this work could be to initialize network weights according to the learned distribution for  $W^*$ . Our preliminary results for this approach seem promising, but more experimentation must be done before we can reach precise conclusions. Another extension could be to apply this method multiple times over patches within an image, e.g. as proposed by Isola et al. [26]. We believe that the inductive benefits of convolutional neural networks will have significant impact in future sensing problems of various types.

## Acknowledgements

This research has been supported by NSF Grants CCF 1422549, 1618689, DMS 1723052, ARO YIP W911NF-14-1-0258 and research gifts by Google, Western Digital and NVIDIA.

## References

- [1] Alekh Agarwal, Sahand Negahban, and Martin J Wainwright. Fast global convergence rates of gradient methods for high-dimensional statistical recovery. In *Advances in Neural Information Processing Systems*, pages 37–45, 2010.
- [2] Nasir Ahmed, T\_ Natarajan, and Kamisetty R Rao. Discrete cosine transform. *IEEE transactions on Computers*, 100(1):90–93, 1974.
- [3] Muhammad Asim, Fahad Shamshad, and Ali Ahmed. Solving bilinear inverse problems using deep generative priors. *CoRR*, abs/1802.04073, 2018.
- [4] Francis Bach, Rodolphe Jenatton, Julien Mairal, Guillaume Obozinski, et al. Optimization with sparsity-inducing penalties. *Foundations and Trends® in Machine Learning*, 4(1):1–106, 2012.
- [5] Richard G Baraniuk, Volkan Cevher, Marco F Duarte, and Chinmay Hegde. Model-based compressive sensing. *IEEE Transactions on Information Theory*, 56(4):1982–2001, 2010.
- [6] Peter J Bickel, Ya’acov Ritov, Alexandre B Tsybakov, et al. Simultaneous analysis of lasso and dantzig selector. *The Annals of Statistics*, 37(4):1705–1732, 2009.
- [7] Ashish Bora, Ajil Jalal, Eric Price, and Alexandros G Dimakis. Compressed sensing using generative models. *arXiv preprint arXiv:1703.03208*, 2017.
- [8] Emmanuel J Candès, Justin Romberg, and Terence Tao. Robust uncertainty principles: Exact signal reconstruction from highly incomplete frequency information. *IEEE Transactions on information theory*, 52(2):489–509, 2006.
- [9] Emmanuel J Candes, Justin K Romberg, and Terence Tao. Stable signal recovery from incomplete and inaccurate measurements. *Communications on pure and applied mathematics*, 59(8):1207–1223, 2006.
- [10] Emmanuel J Candes and Terence Tao. Decoding by linear programming. *IEEE transactions on information theory*, 51(12):4203–4215, 2005.
- [11] Jen-Hao Rick Chang, Chun-Liang Li, Barnabás Póczos, B. V. K. Vijaya Kumar, and Aswin C. Sankaranarayanan. One network to solve them all - solving linear inverse problems using deep projection models. *CoRR*, abs/1703.09912, 2017.
- [12] Guang-Hong Chen, Jie Tang, and Shuai Leng. Prior image constrained compressed sensing (piccs): a method to accurately reconstruct dynamic ct images from highly undersampled projection data sets. *Medical physics*, 35(2):660–663, 2008.
- [13] Ingrid Daubechies. Orthonormal bases of compactly supported wavelets. *Communications on pure and applied mathematics*, 41(7):909–996, 1988.
- [14] Akshat Dave, Anil Kumar Vadathya, Ramana Subramanyam, Rahul Baburajan, and Kaushik Mitra. Solving inverse computational imaging problems using deep pixel-level prior. *arXiv preprint arXiv:1802.09850*, 2018.
- [15] David L Donoho. Compressed sensing. *IEEE Transactions on information theory*, 52(4):1289–1306, 2006.
- [16] Marco F Duarte, Mark A Davenport, Dharmpal Takhar, Jason N Laska, Ting Sun, Kevin F Kelly, and Richard G Baraniuk. Single-pixel imaging via compressive sampling. *IEEE signal processing magazine*, 25(2):83–91, 2008.
- [17] Armin Eftekhari and Michael B Wakin. New analysis of manifold embeddings and signal recovery from compressive measurements. *Applied and Computational Harmonic Analysis*, 39(1):67–109, 2015.

- [18] David Eigen and Rob Fergus. Predicting depth, surface normals and semantic labels with a common multi-scale convolutional architecture. In *Proceedings of the IEEE International Conference on Computer Vision*, pages 2650–2658, 2015.
- [19] Alyson K Fletcher and Sundeep Rangan. Inference in deep networks in high dimensions. *arXiv preprint arXiv:1706.06549*, 2017.
- [20] Ian Goodfellow, Jean Pouget-Abadie, Mehdi Mirza, Bing Xu, David Warde-Farley, Sherjil Ozair, Aaron Courville, and Yoshua Bengio. Generative adversarial nets. In *Advances in neural information processing systems*, pages 2672–2680, 2014.
- [21] Aditya Grover and Stefano Ermon. Amortized variational compressive sensing. 2018.
- [22] Paul Hand and Vladislav Voroninski. Global guarantees for enforcing deep generative priors by empirical risk. *arXiv preprint arXiv:1705.07576*, 2017.
- [23] Chinmay Hegde and Richard G Baraniuk. Signal recovery on incoherent manifolds. *IEEE Transactions on Information Theory*, 58(12):7204–7214, 2012.
- [24] Chinmay Hegde, Michael Wakin, and Richard Baraniuk. Random projections for manifold learning. In *Advances in neural information processing systems*, pages 641–648, 2008.
- [25] AD Hoover, Valentina Kouznetsova, and Michael Goldbaum. Locating blood vessels in retinal images by piecewise threshold probing of a matched filter response. *IEEE Transactions on Medical imaging*, 19(3):203–210, 2000.
- [26] Phillip Isola, Jun-Yan Zhu, Tinghui Zhou, and Alexei A Efros. Image-to-image translation with conditional adversarial networks. *arXiv preprint*, 2017.
- [27] Stefan Jaeger, Sema Candemir, Sameer Antani, Yi-Xiáng J Wáng, Pu-Xuan Lu, and George Thoma. Two public chest x-ray datasets for computer-aided screening of pulmonary diseases. *Quantitative imaging in medicine and surgery*, 4(6):475, 2014.
- [28] Maya Kabkab, Pouya Samangouei, and Rama Chellappa. Task-aware compressed sensing with generative adversarial networks. *arXiv preprint arXiv:1802.01284*, 2018.
- [29] Diederik P Kingma and Max Welling. Auto-encoding variational bayes. *arXiv preprint arXiv:1312.6114*, 2013.
- [30] Alex Krizhevsky, Ilya Sutskever, and Geoffrey E Hinton. Imagenet classification with deep convolutional neural networks. In *Advances in neural information processing systems*, pages 1097–1105, 2012.
- [31] Yann LeCun, Léon Bottou, Yoshua Bengio, and Patrick Haffner. Gradient-based learning applied to document recognition. *Proceedings of the IEEE*, 86(11):2278–2324, 1998.
- [32] Ziwei Liu, Ping Luo, Xiaogang Wang, and Xiaoou Tang. Deep learning face attributes in the wild. In *Proceedings of International Conference on Computer Vision (ICCV)*, 2015.
- [33] Po-Ling Loh and Martin J Wainwright. High-dimensional regression with noisy and missing data: Provable guarantees with non-convexity. In *Advances in Neural Information Processing Systems*, pages 2726–2734, 2011.
- [34] Michael Lustig, David Donoho, and John M Pauly. Sparse mri: The application of compressed sensing for rapid mr imaging. *Magnetic resonance in medicine*, 58(6):1182–1195, 2007.
- [35] Morteza Mardani, Hatef Monajemi, Vardan Papyan, Shreyas Vasanaawala, David Donoho, and John Pauly. Recurrent generative adversarial networks for proximal learning and automated compressive image recovery. *arXiv preprint arXiv:1711.10046*, 2017.

- [36] Sahand Negahban, Bin Yu, Martin J Wainwright, and Pradeep K Ravikumar. A unified framework for high-dimensional analysis of  $m$ -estimators with decomposable regularizers. In *Advances in Neural Information Processing Systems*, pages 1348–1356, 2009.
- [37] Adam Paszke, Sam Gross, Soumith Chintala, Gregory Chanan, Edward Yang, Zachary DeVito, Zeming Lin, Alban Desmaison, Luca Antiga, and Adam Lerer. Automatic differentiation in pytorch. 2017.
- [38] F. Pedregosa, G. Varoquaux, A. Gramfort, V. Michel, B. Thirion, O. Grisel, M. Blondel, P. Prettenhofer, R. Weiss, V. Dubourg, J. Vanderplas, A. Passos, D. Cournapeau, M. Brucher, M. Perrot, and E. Duchesnay. Scikit-learn: Machine learning in Python. *Journal of Machine Learning Research*, 12:2825–2830, 2011.
- [39] Saad Qaisar, Rana Muhammad Bilal, Wafa Iqbal, Muqaddas Naureen, and Sungyoung Lee. Compressive sensing: From theory to applications, a survey. *Journal of Communications and networks*, 15(5):443–456, 2013.
- [40] Alec Radford, Luke Metz, and Soumith Chintala. Unsupervised representation learning with deep convolutional generative adversarial networks. *arXiv preprint arXiv:1511.06434*, 2015.
- [41] Viraj Shah and Chinmay Hegde. Solving linear inverse problems using gan priors: An algorithm with provable guarantees. *arXiv preprint arXiv:1802.08406*, 2018.
- [42] Robert Tibshirani. Regression shrinkage and selection via the lasso. *Journal of the Royal Statistical Society. Series B (Methodological)*, pages 267–288, 1996.
- [43] Tijmen Tieleman and Geoffrey Hinton. Lecture 6.5-rmsprop: Divide the gradient by a running average of its recent magnitude. *COURSERA: Neural networks for machine learning*, 4(2):26–31, 2012.
- [44] Subarna Tripathi, Zachary C Lipton, and Truong Q Nguyen. Correction by projection: Denoising images with generative adversarial networks. *arXiv preprint arXiv:1803.04477*, 2018.
- [45] Joel A Tropp. Just relax: Convex programming methods for identifying sparse signals in noise. *IEEE transactions on information theory*, 52(3):1030–1051, 2006.
- [46] Dmitry Ulyanov, Andrea Vedaldi, and Victor Lempitsky. Deep image prior. *arXiv preprint arXiv:1711.10925*, 2017.
- [47] Aaron Van Den Oord, Sander Dieleman, Heiga Zen, Karen Simonyan, Oriol Vinyals, Alex Graves, Nal Kalchbrenner, Andrew Senior, and Koray Kavukcuoglu. Wavenet: A generative model for raw audio. *arXiv preprint arXiv:1609.03499*, 2016.
- [48] Zhou Wang, Alan C Bovik, Hamid R Sheikh, and Eero P Simoncelli. Image quality assessment: from error visibility to structural similarity. *IEEE transactions on image processing*, 13(4):600–612, 2004.
- [49] F Wasilewski. Pywavelets: Discrete wavelet transform in python, 2010.
- [50] David W Winters, Barry D Van Veen, and Susan C Hagness. A sparsity regularization approach to the electromagnetic inverse scattering problem. *IEEE transactions on antennas and propagation*, 58(1):145–154, 2010.

## 6 Appendix

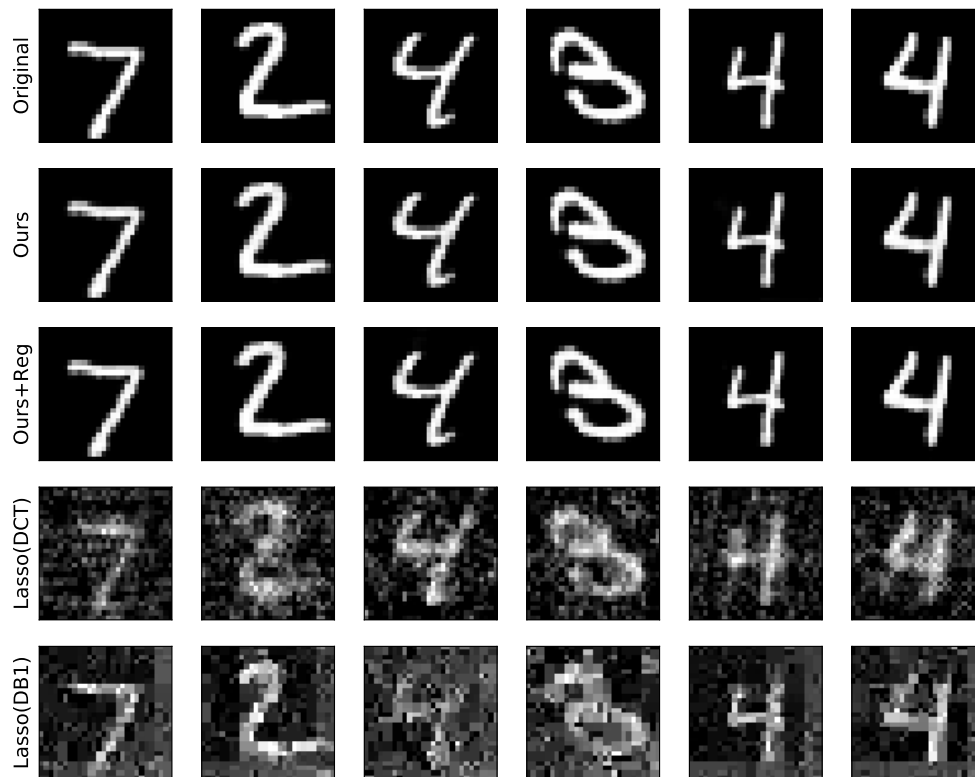


Figure 5: Reconstruction results on MNIST with  $m = 200$  measurements (of  $n = 784$  dimensional vector). We show original images (top row), reconstructions by our algorithm (second row), our algorithm with our regularizer (third row), Lasso with DCT and DB1 wavelet basis (last two rows).

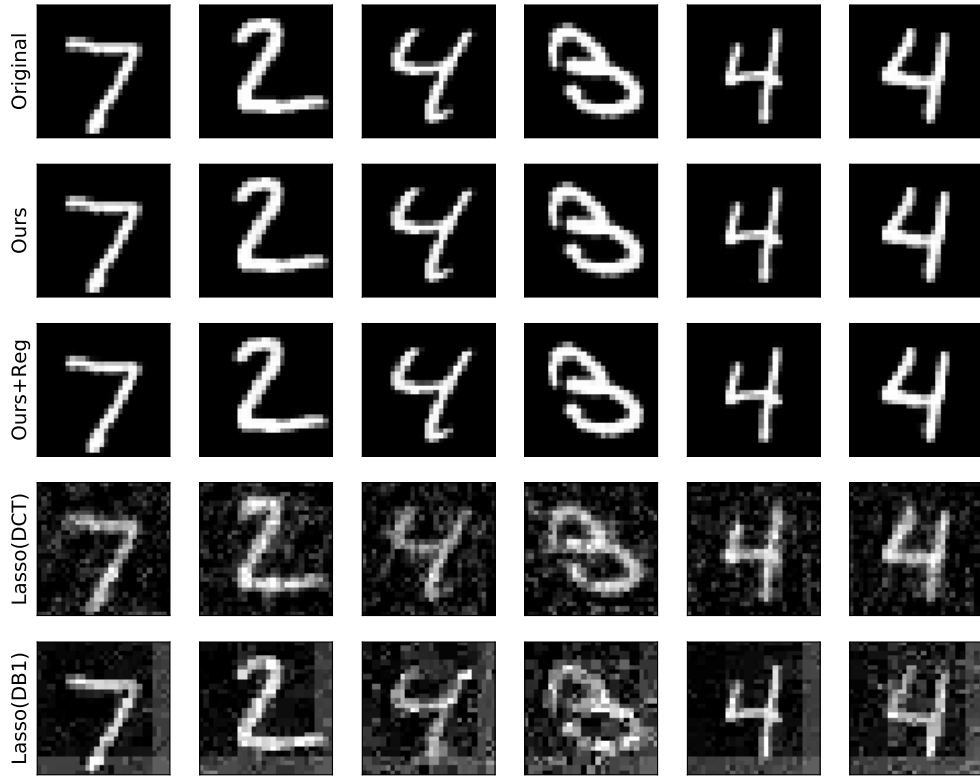


Figure 6: Reconstruction results on MNIST with  $m = 300$  measurements (of  $n = 784$  dimensional vector). We show original images (top row), reconstructions by our algorithm (second row), our algorithm with our regularizer (third row), Lasso with DCT and DB1 wavelet basis (last two rows).

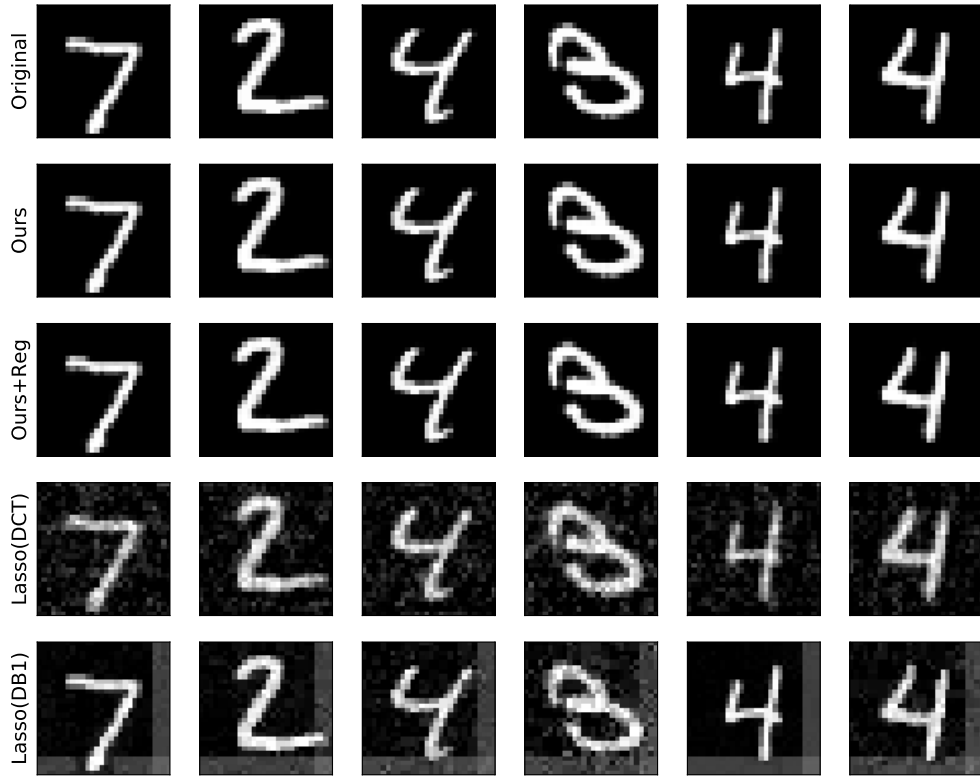


Figure 7: Reconstruction results on MNIST with  $m = 400$  measurements (of  $n = 784$  dimensional vector). We show original images (top row), reconstructions by our algorithm (second row), our algorithm with our regularizer (third row), Lasso with DCT and DB1 wavelet basis (last two rows).

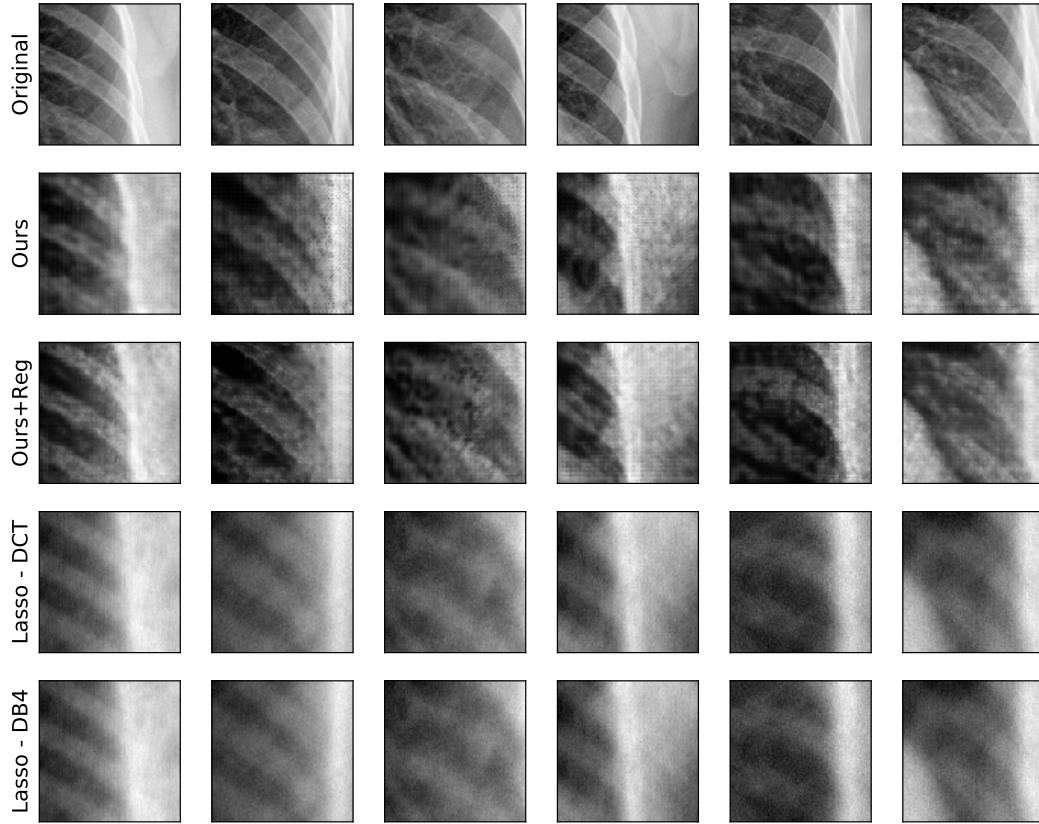


Figure 8: Reconstruction results on X-Rays with  $m = 1000$  measurements (of  $n = 65536$  dimensional vector). We show original images (top row), reconstructions by our algorithm (second row), our algorithm with our regularizer (third row), Lasso with DCT basis (fourth row), and Lasso with DB4 wavelet basis (last row).



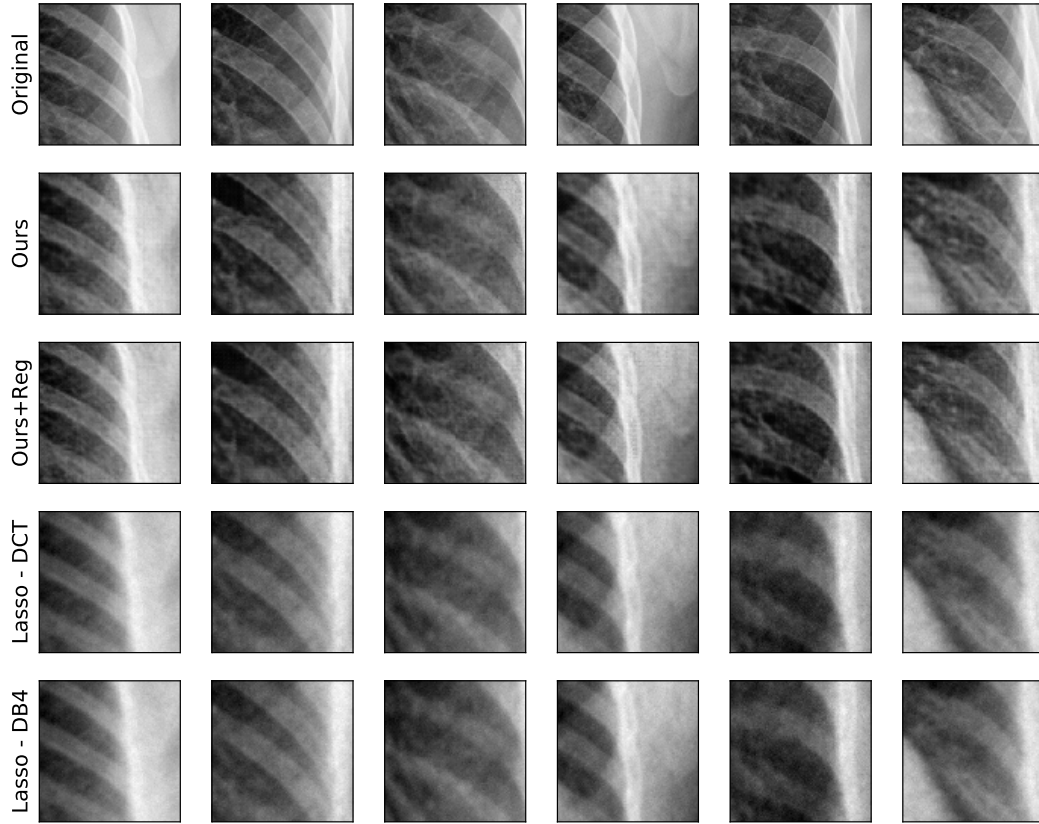


Figure 9: Reconstruction results on X-Rays with  $m = 4000$  measurements (of  $n = 65536$  dimensional vector). We show original images (top row), reconstructions by our algorithm (second row), our algorithm with our regularizer (third row), Lasso with DCT basis (fourth row), and Lasso with DB4 wavelet basis (last row).

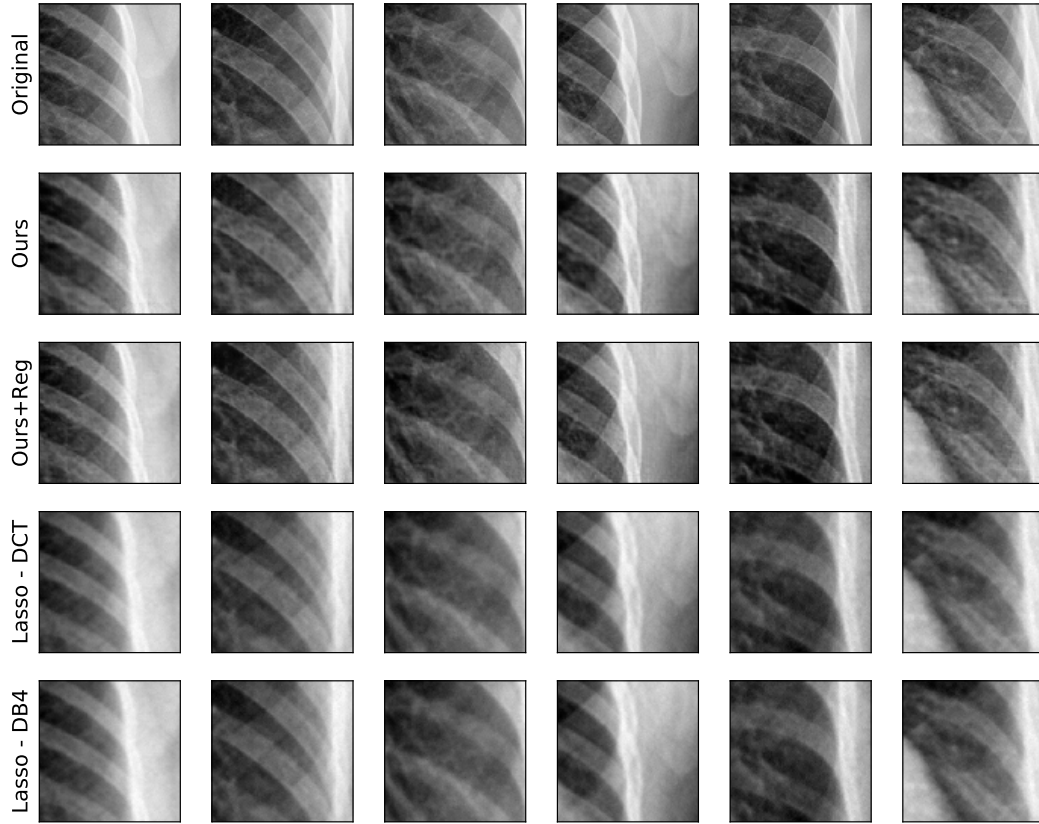


Figure 10: Reconstruction results on X-Rays with  $m = 8000$  measurements (of  $n = 65536$  dimensional vector). We show original images (top row), reconstructions by our algorithm (second row), our algorithm with our regularizer (third row), Lasso with DCT basis (fourth row), and Lasso with DB4 wavelet basis (last row).